ACS APPLIED MATERIALS & INTERFACES

LETTER

www.acsami.org

Design and Development of Novel Linker for PbS Quantum Dots/TiO_2 Mesoscopic Solar cell

Lioz Etgar,*[,†] JinHyung Park,[‡] Claudia Barolo,*[,‡] Md. K. Nazeeruddin,[†] Guido Viscardi,[‡] and Michael Graetzel[†]

[†]Laboratoire de Photonique et Interfaces, Institut des Sciences et Ingénierie Chimiques, Ecole Polytechnique Fédérale de Lausanne (EPFL), Station 6, CH-1015 Lausanne, Switzerland

[‡]Dipartimento di Chimica Generale e Chimica Organica, NIS Centre of Excellence, Università di Torino, Corso Massimo D'Azeglio 48, I-10125 Torino, Italy

Supporting Information

ABSTRACT: A novel bifunctional linker molecule, bis(4-mercaptophenyl)phosphinic acid, is designed to be used in a QDs solar cells. The linker anchors to TiO_2 mesoporous film through the phosphinic acid functional group and to the PbS QDs through the two thiol groups. The way of attachment of this new linker molecule in a photovoltaic PbS QDs/TiO_2 mesoporous device was studied by FTIR measurements. The photovoltaic performance of this new linker in a heterojunction PbS QDs solar cell show high V_{oc} relative to QDs based solar cells, which will allow to receive high power conversion efficiency using this novel designed linker. This novel bifunctional linker molecule should pave the way for enhancing binding strength, and efficiency of QDs solar cells compared to the state-of-the-art linkers.

KEYWORDS: quantum dots, bifunctional molecular linker, heterojunction solar cells, phosphinic acid, PbS, mesoporous TiO_2

INTRODUCTION

Dye-sensitized solar cells (DSSC), which yield 11% power conversion efficiency, are low cost alternative to traditional silicon solar cells.[1] Upon illumination, the dye absorbs photons, and goes to excited state generating electron and hole pairs. The electrons are injected into the TiO_2 conduction band and diffuse to the front contact; simultaneously, the holes are injected into redox couple. Replacing the dye molecule by inorganic quantum dots (QDs), which have larger optical cross section compared to transition metal complexes, coupled with tunability of their band gap due to quantum size effect,[2−4] has attracted lot of attention as photon absorbing material. QDs have been intensively investigated in a variety of photovoltaic device architectures, including nanocrystal (NC)-polymer hybrid solar cells, NC Schottky solar cells, NC-sensitized titanium dioxide (TiO_2) solar cells, and NC hybrid bilayer solar cells.[5−10] To attach the QDs to the TiO_2 nanoparticle (NPs) mesoporous film in the photovoltaic device, we have to use a linker molecule. Several commercially available linker molecules such as mercaptopropionic acid, ethan dithiol, thioglycolic acid, cysteine, thiolacetic acid, mercaptohexadecanoic acid, and benzenethiol derivatives have been used.[11−13] However, to date, no tailored linker molecules were described in literature.

In this work, we report on a specifically designed bifunctional linker molecule bis(4-mercaptophenyl)phosphinic acid (BMPA, see figure 1), which anchors to TiO_2 mesoporous film through the phosphinic acid functional group and PbS QDs through the two thiol groups. The short bridge due the presence of the aromatic rings should provide better conductivity for electrons through the QDs film. A detailed study of the attachment of this new linker molecule in a photovoltaic PbS QDs/TiO_2 mesoporous device was made. Preliminary results showing the photovoltaic performance of this new linker in a heterojunction PbS QDs solar cell are presented.

EXPERIMENTAL SECTION

Chemicals and Materials. All reagents and solvents were obtained from commercial suppliers at the highest purity grade and used without further purification. Extracts were dried over Na_2SO_4 and filtered before removal of the solvent by evaporation. Reactions were performed under nitrogen in oven-dried glassware and monitored by thin layer chromatography using UV light (254 and 365 nm) as visualizing agent. Flash chromatography was performed with Merck grade 9385 silica gel 230−400 mesh (60 Å).

NMR spectra were recorded on a Jeol EX400 NMR spectrometer or on a Bruker AC-200 instrument in DMSO-d_6 using the DMSO signal as a reference. NMR signals are described by use of s for singlet, d for doublet, t for triplet, m for multiplet. Mass spectra were recorded on a Thermo Finnigan Advantage Max Ion Trap Spectrometer equipped with an electrospray ion source (ESI) in negative ion acquiring mode.

Synthesis. The synthetic pathway followed for the preparation of BMPA molecule is shown in scheme 1. A simple synthetic method for the preparation of bisphenyl phosphinic acids has been recently reported.[14,15] This procedure, based on the use of n-BuLi and $Cl_2P(O)NMe_2$, is reliable in the case of 4-substitued phenyl derivatives with functional groups such as $-CH_3$, $-OCH_3$ $-CF_3$, but cannot be applied in the case of -SH, due to the reactivity of thiol group. A protective group resistant to n-BuLi, such as SCH_3, should be then used. The application of the standard procedure to 4-bromothioanisole **1** gave the phosphinic acid **2** in good yield. Deprotection of a methylthio group to afford the corresponding thiol can be achieved by reaction with either sodium t-butylthiolate in DMF[16a,b] or m-CPBA/TFAA,[17] via sulfoxide intermediate **3**. However, the application of the published standard protocols to **2** afforded a complex mixture in which the predominant product is the corresponding sulfone,[18] not easy to convert in

Received: June 23, 2011
Accepted: August 4, 2011
Published: August 04, 2011

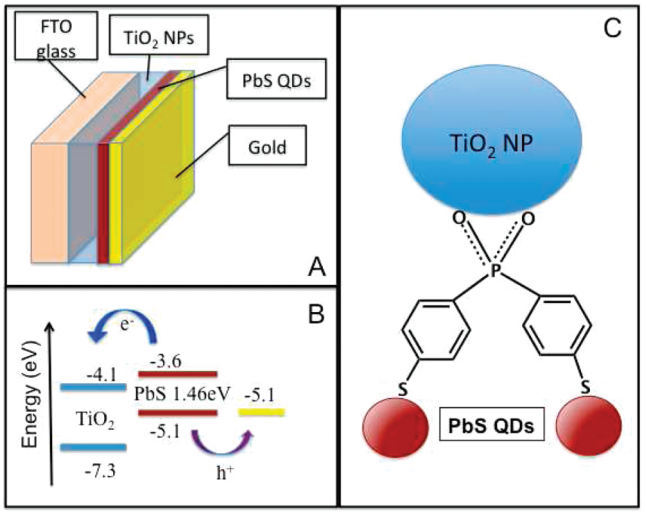

Figure 1. (A) Architecture of the PbS QD/mesoscopic TiO_2 photovoltaic device, the light is incident through the glass. (B) Energy level diagram of the solar cell for PbS quantum dots with E_g of 1.46 eV.[19,20] (C) The way the BMPA molecule is linked between the TiO_2 NP and the PbS QDs.

Scheme 1. Synthesis of Bis(4-mercaptophenyl)phosphinic Acid (5)

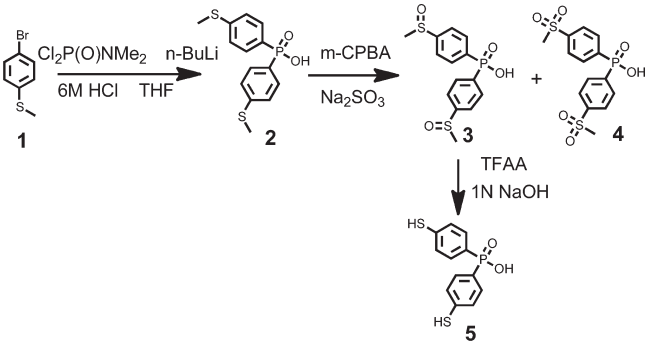

SH group. To obtain the needed intermediate **3**, we chose to carefully control the oxidation step through an accurate setup of both reagent ratio (use of freshly crystallized m-CPBA) and reaction temperature. Finally, the desired phosphinic acid **5** was obtained by the action of trifluoroacetic anhydride on **3**. See the Supporting Information for detailed characterization data.

Methods and Device Fabrication. Colloidal PbS NCs capped with oleic acid were purchased from Evident technologies and stored in nitrogen-filled glovebox.

During device fabrication, a thin blocking layer of compact TiO_2 was first deposited by spray pyrolysis onto a precleaned FTO glass substrate using a solution of titanium diisopropoxide bis(acetylacetonate) in ethanol as precursor. Subsequently, a porous TiO_2 layer was deposited by doctor blading technique from a dilute aqueous paste containing a mixture of 18 nm sized TiO_2 particles and 500 nm sized polystyrene beads. The polystyrene was burned during the subsequent sintering step performed for 30 min at 450 °C producing macropores of 200 nm pore size. In addition, the 500 ± 50 nm thick titania film contained 23 nm-sized mesopores was generated from the TiO_2 nanoparticle network.

The PbS QDs were subsequently deposited layer by layer on the porous TiO_2 film by spin coating a 50 mg mL^{-1} solution in octane. Each layer was cast at a spinning rate of 2500 rpm applied for 10 s and treated thereafter briefly with a solution of 2.3 mM BMPA in methanol using again 2500 rpm rotational speed for 10 s. This treatment displaced the oleic acid ligand and rendered the QD insoluble, which allowed thin films of 300 nm thicknesses to be created using 12 successive deposition cycles. Each layer was rinsed with anhydrous methanol and anhydrous octane to remove excess of BMPA and PbS QDs. Finally, a gold back contact of ca. 100 nm thick, was deposited by evaporation through a shadow mask. The device was then completed by encapsulation in Argon atmosphere. The encapsulation of the device was made by placing 2 mm glass on top of the active area of the device using a piece of hot melt Surlyn (25 μm thick) as a spacer. After encapsulation the device was stable under air.

Photovoltaic Characterization. Photovoltaic measurements employed an AM 1.5 solar simulator equipped with a 450W xenon lamp (Model No. 81172, Oriel). Its power output was adjusted to match AM 1.5 global sunlight (100 mW/cm^2) by using a reference Si photodiode equipped with an IR-cutoff filter (KG-3, Schott) in order to reduce the mismatch between the simulated light and AM 1.5 (in the region of 350−750 nm) to less than 2% with measurements verified at two PV calibration laboratories [ISE (Germany), NREL (USA)]. $I-V$ curves were obtained by applying an external bias to the cell and measuring the generated photocurrent with a Keithley model 2400 digital source meter. The voltage step and delay time of photocurrent were 10 mV and 40 ms, respectively. A similar data acquisition system was used to determine the monochromatic incident photon- to-electric current conversion efficiency. Under full computer control, light from a 300 W xenon lamp (ILC Technology, U.S.A.) was focused through a Gemini-180 double monochromator (Jobin Yvon Ltd., U.K.) onto the photovoltaic cell under test. The monochromator was incremented through the visible spectrum to generate the IPCE (λ) as defined by IPCE (λ)) = 12400($J_{sc}/\lambda\varphi$), where λ is the wavelength, J_{sc} is short-circuit photocurrent density (mA cm^{-2}), and φ is the incident radiative flux (mW cm^{-2}). Photovoltaic performance was measured by using a metal mask with an aperture area of 0.18 cm^2.

Fourier Transform Infrared (FTIR) Measurements. FTIR measurements were performed with a Digilab FTS 7000 Series spectrometer, using 64 scans with a 2 cm^{-1} resolution step. The pure BMPA was recorded in a solid-phase powder using an ATR-FTIR Shimadzu spectrometer 8400. The ATR data reported here was taken with the "Golden Gate" diamond-anvil ATR accessory.

RESULTS AND DISCUSSION

Mesoscopic PbS/TiO_2 solar cells were made using the BMPA linker. The bottom layer of the device is composed of compact and mesoscopic TiO_2 layers acting as electron collectors. Light is absorbed by the 1.46 eV band gap PbS QDs with Au as the top contact without additional electron blocking layers. (See Figure 1A). The energy level diagram[19,20] of the Solid State QDs Solar Cell is shown in figure 1B; the conduction and valence bands of the 1.46 eV PbS QDs permit electron injection and hole transportation to the TiO_2 and the gold respectively.

The PbS QDs were attached to the TiO_2 NPs film by the BMPA linker; the phosphinic acid functional group is attached to the TiO_2 NPs film while the thiol groups are attached to the PbS QDs (Figure 1C). To confirm the chemical attachment of the BMPA to the titania surface, Fourier transform infrared (FTIR) spectra were recorded (Figure 2) for pure BMPA (red), TiO_2 NPs film without the treatment of BMPA (black), BMPA attached to TiO_2 NPs film (green), and complete PbS QDs solar cell using the BMPA as a linker (blue).

The stretching, bending and contraction of the aromatic rings are assigned to the frequency range of 900 to 1100 cm^{-1}. In addition, the Phosphorus aromatic ring mode is assigned to the band at 1092 cm^{-1}.[21] These modes can be recognized for all

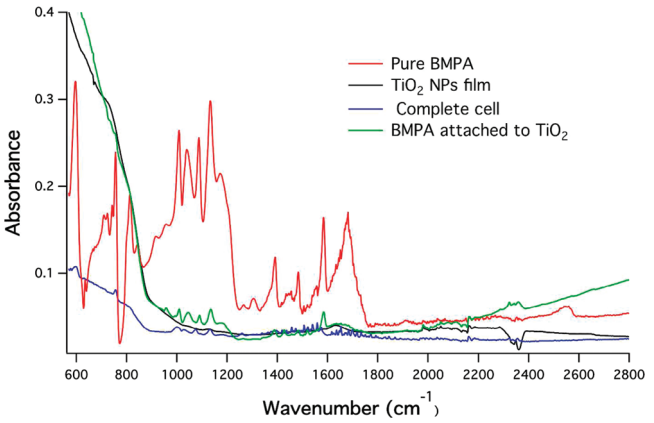

Figure 2. FTIR spectra of the pure Bis(4-mercaptophenyl) phosphinic acid -BMPA (red), TiO_2 NPs film without BMPA treatment (black), BMPA attached to TiO_2 NPs film (green), and the complete cell (blue).

Table 1. PV Performance of Different BMPA Concentrations Used in the Mesoscopic PbS QDs/TiO_2 Solar Cell[a]

BMPA concentration (mM)	V_{oc} (mV)	J_{sc} (mA/cm^2)	FF %	% efficiency @ 1.5AM
0	495	0.76 ± 0.06	29	0.11
2.3	580	1.55 ± 0.06	37	0.33
11	572	1.69 ± 0.07	34	0.33

[a] The measurements were done using a metal mask with an aperture area of 0.18 cm^2.

spectra except the TiO_2 NPs film without the BMPA treatment spectrum. This observation is evidence that the BMPA is attaching to the TiO_2 surface.

Moreover, the P═O mode of the phosphinic acid appears at 1200 cm^{-1} for the pure BMPA, but it disappears once the BMPA is attached to the TiO_2 surface. The abstention of this peak is an additional proof of the chemical attachment of the BMPA to the TiO_2 surface through the phosphinic acid. According to the literature the possible bonding modes of the phosphoryl oxygens to the TiO_2 surface are tridentate or bidentate.[21] In our case, the BMPA molecule has two aromatic rings; as a result the tridenate bonding mode of the phosphoryl oxygens to the TiO_2 surface cann't accur, because it requires three oxygens connected to the TiO_2 surface. As a result the bidentate bonding mode is the preferred attachment of the phosphoryl oxygens to the TiO_2 surface (see Figure 1C).

The pure BMPA spectrum exhibits hydrogen vibrations related to the aromatic rings at the range of 1300 to 1500 cm^{-1}.[21] The S−H stretching band at 2590 cm^{-1} appears in the BMPA spectrum while this streching band is weak in the BMPA attached to the TiO_2 surface spectrum. The attachment of the BMPA to the TiO_2 surface without the presence of the PbS QDs may cause the thiol groups also to be connected to the TiO_2 surface; as a result the S−H stretching band is weak. The S−H stretching band completely disappears once the BMPA is accosiated with the PbS QDs.

Table 1 shows different concentrations of BMPA used in the mesoscopic PbS QDs/TiO_2 photovoltaic device. It can be seen that the increasing of the BMPA concentration does not affect the PV performance (2.3 mM and 11 mM). We assume that because of the low solubility of the BMPA not all the oleic acid previously capped the PbS QDs are exchanged by the BMPA linker (see Table 1 when no BMPA was used), hence the current

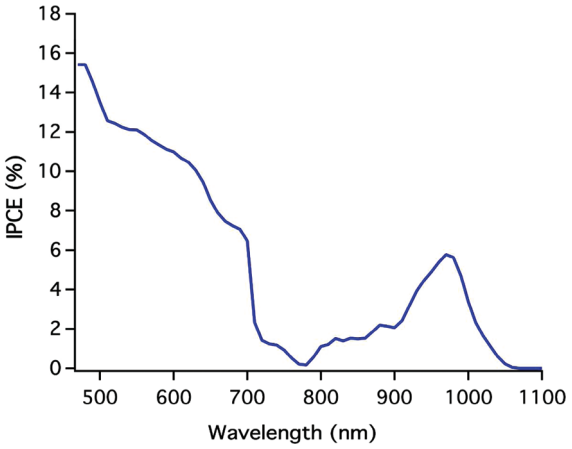

Figure 3. Spectral response curve of the photocurrent for the mesoscopic PbS QDs/TiO_2 photovoltaic device. The incident photon to current conversion efficiency is plotted as a function of wavelength of the incident light.

density of the device is still low. However, the high Voc relative to QDs based solar cells is promising. We suggest that a monolayer of the BMPA linker, which adsorbed on the TiO_2 surface, suppressed the back transfer electrons from the conduction band of the TiO_2 to the valence band of the QDs, as a result the voltage of the solar cell can be increased. Higher Voc will allow receiving high power conversion efficiency using new designed linker of this type.

Figure 3 shows the incident photon to current conversion efficiency (IPCE), or external quantum efficiency, specifies the ratio of extracted electrons to incident photons at a given wavelength. The IPCE spectrum is plotted as a function of wavelength of the light. The PbS QD/mesoscopic TiO_2 photovoltaic device shows a response from the visible through the near-infrared (NIR), the IPCE reaching its maximum of 15.5% at 470 nm. The excitonic peak of the PbS QDs was red-shifted as a result of the device preparation. The excitonic peak can be observed at 970 nm corresponding to IPCE of 6%. Integration of the IPCE spectrum over the AM1.5 solar emission yields a photocurrent density of 2.1 mA/cm^2 in reasonable agreement with the measured value.

The preliminary photovoltaic results using the low concentration of BMPA showing open circuit voltage (V_{oc}) of 0.58 V, a short circuit current density (J_{sc}) of 1.55 mA cm^{-2} and a fill factor of 37% corresponding to a power conversion efficiency (PCE) of 0.33% under AM1.5. Although the photovoltaic performance using this new linker is still lower respect to the classical available organic linkers,[11−13,20] this particular structure showed a potential to receive high power conversion efficiency. Further work is underway to improve the BMPA solubility and to increase the total power conversion efficiency.

CONCLUSIONS

In this work, we presented a novel bifunctional molecule (BMPA) used as a linker for solid-state PbS QDs/TiO_2 solar cells. This new linker was designed and synthesized especially to connect the PbS QDs to the TiO_2 surface. The BMPA molecule has phosphonic acid functional group known to have excellent affinity to TiO_2 surface, the aromatic rings exhibit very good electron conductivity through the QDs film and the thiol groups should attached to the QDs surface replacing the oleic acid ligands. FTIR measurements showed the attachment of this BMPA molecule to the

TiO_2 NPs surface and to the PbS QDs. Mesoscopic PbS QDs/TiO_2 solar cells containing this novel linker were made showing the potential of this new linker in QDs solar cells devices.

■ ASSOCIATED CONTENT

Supporting Information. Full experimental of the synthesis of the BMPA molecule includes: NMR, Mass spectra and UV measurements. This material is available free of charge via the Internet at http://pubs.acs.org/.

■ AUTHOR INFORMATION

Corresponding Author

*E-mail: lioz.etgar@epfl.ch (L.E.); claudia.barolo@unito.it (C.B.). Fax: +41 21 6934111 (L.E.); +390116707596 (C.B.). Tel: +41 21 6936169 (L.E.); +390116707596 (C.B.).

■ ACKNOWLEDGMENT

Authors acknowledge financial support of this work by the EU project "Innovasol" grant agreement number 227057-2. L.E. acknowledges the Marie Curie Actions—Intra-European Fellowships (FP7-PEOPLE-2009-IEF) under grant agreement n° 252228, project "Excitonic Solar Cell". J.P., C.B., and G.V. thank Compagnia di San Paolo and Fondazione CRT for continuous equipment supply.

■ REFERENCES

(1) Reiko, Y. O.; Shigeru, N.; Masahiro, M.; Masaki, O.; Yusuke, S.; Kazuhiro, N. *Appl. Phys. Lett.* **2009**, *94*, 073308.
(2) Kamat, P. V. *J. Phys. Chem. C* **2008**, *112*, 18737.
(3) Huynh, W. U.; Dittmer, J. J.; Alivisatos, A. P. *Science* **2002**, *295*, 2425.
(4) Gur, I.; Fromer, N. A.; Geier, M. I.; Alivisatos, A. P. *Science* **2005**, *310*, 462.
(5) Jonhston, K. W.; Pattantyus-Abraham, A. G.; Clifford, J. P.; Myrskog, S. H.; MacNeil, D.; Levina, L.; Sargent, E. H. *Appl. Phys. Lett.* **2008**, *92*, 151115.
(6) Luther, J. M.; Law, M.; Beard, M. C.; Song, Q.; Reese, M. O.; Ellingson, R. J.; Nozik, A. J. *Nano lett.* **2008**, *8*, 3488.
(7) Ma, W.; Luther, J. M.; Zheng, H.; Wu, Y.; Alivisatos, A. P. *Nano Lett.* **2009**, *9*, 1699.
(8) Lee, H.; Leventis, H. C.; Moon, S.-J.; Chen, P.; Ito, S.; Haque, S. A.; Torres, T.; Nüesch, F.; Geiger, T.; Zakeeruddin, S. M.; Grätzel, M; Nazeeruddin, M. K. *Adv. Funct. Mater.* **2009**, *19*, 2735.
(9) Zhang, S.; Cyr, P. W.; McDonald, S. A.; Konstantatos, G.; Sargent, E. H. *Appl. Phys. Lett.* **2005**, *87*, 233101.
(10) Seo, J.; Kim, S. J.; Kim, W. J.; Singh, R.; Samoc, M.; Cartwright, A. N.; Prasad, P. N. *Nanotechnology* **2009**, *20*, 95202.
(11) Menny, S.; Sven, R.; Idan, H.; Shay, Y.; Arie, Z. *J. Am. Chem. Soc.* **2009**, *131*, 9876–9877.
(12) Mora-Sero, I.; Gimenez, S.; Moehl, T.; Fabregat-Santiago, F.; Lana-Villareal, T.; Gomez, R.; Bisquert, J. *Nanotechnology* **2008**, *19*, 424007.
(13) Robel, I.; Subramanian, V.; Kuno, M.; Kamat, P. V. *J Am. Chem. Soc.* **2006**, *128*, 2385.
(14) Driver, T. G.; Harris, J. R.; Woerpel, K. A. *J. Am. Chem. Soc.* **2007**, *129*, 3836–3837.
(15) Watson, D. A.; Chiu, M.; Bergman, R. G. *Organometallics* **2006**, *25*, 4731–4733.
(16) (a) Pinehart, A.; Dallaire, C.; Van, B. A.; Gingras, M. *Tetrahedron Lett.* **1999**, *40*, 5479–5482. (b) Gallardo-Godoyyatt, A.; Torres-Altoro, M. I.; White, K. J.; Barker, E. L.; Nichols, D. E. *Bioorg. Med. Chem.* **2007**, *15*, 305–311.
(17) Wyatt, P.; Hudson, A. *Org. Biomol. Chem.* **2004**, *2*, 1528–1530.
(18) Jing, Y.; Huang, X. *Tetraheron Lett.* **2004**, *45*, 4615–4618.
(19) Hyun, B.-R.; Zhong, Y.-W.; Bartnik, A. C.; Sun, L.; Abruna, H. D.; Wise, F. W.; Goodreau, J. D.; Matthews, J. R.; Leslie, T. M.; Borrelli, N. F. *ACS Nano* **2008**, *2*, 2206.
(20) Aaron, D.; Barkhouse, R.; Debnath, R.; Kramer, J. I; Zhitomirsky, D; Pattantyus-Abraham, A. G.; Levina, L.; Etgar, L.; Grätzel, M.; Sargent, E. H. *Adv. Mater.* **2011**, DOI: 10.1002/adma.201101065.
(21) Guerrero, G.; Mutin, P. H.; Vioux, A. *Chem. Mater.* **2001**, *13* (11), 4367–4373.